Comparison of Experimental and Theoretical Results on Polysilicon Emitter Bipolar Transistors

PETER ASHBURN AND B. SOEROWIRDJO

Abstract—Two types of polysilicon emitter transistors have been fabricated using identical processing except for the surface treatment prior to polysilicon deposition. The first type was given a dip etch in buffered hydrofluoric acid, which was intended to remove any interfacial oxide, while the second type was given an RCA clean, which was intended to grow an interfacial oxide of known thickness. Detailed electrical measurements have been made on these devices including the temperature dependence of the gain over a wide temperature range. The transistors given an RCA clean have gains approximately five times higher than those given an HF etch. In addition, the temperature dependence of the gain is different for the two types, with the HF devices exhibiting a much stronger dependence at high temperatures than the RCA devices. A detailed comparison is made with the theory and it is shown that the characteristics of the HF devices can largely be explained using a transport theory, while those of the RCA devices can be fully explained using a modified tunneling theory.

I. Introduction

POLYCRYSTALLINE silicon is increasingly being used in bipolar integrated-circuit processes for producing self-aligned circuits [1]-[3] with a consequent improvement in both switching speed and packing density. When used in shallow emitter structures the polysilicon also provides a means of obtaining very shallow junctions with very high yields. These high yields result from a reduction in anomalous diffusion effects [4] and in defect generation [5], [6] associated with the high-concentration emitter diffusion [7].

In addition to the preceding advantages, improved gains can be obtained for transistors with polysilicon emitters [8]. Improvements from 3 [9] to 30 [10], [11] have been reported in the literature, and in a previous publication [8], [12] the authors showed that the gain improvement depended strongly on the type of surface treatment given prior to polysilicon deposition. Two alternative theories have been proposed to explain the improved gains obtained for polysilicon emitter transistors. The first was proposed by Ning and Isaac [9]; [13], [14], and explained the improved gains in terms of a shorter hole diffusion coefficient in the polycrystalline part of the emitter than in the single-crystal part. The second was proposed by De Graaff and De Groot [10], and explained the improved gains by tunneling through a thin interfacial oxide layer located between the polysilicon and single-crystal silicon. More recently, Eltoukhy and Roulston have reported [15], [16] on a unified theory which incorporates both these mechanisms in a form suitable for fast numerical solution.

Manuscript received November 30, 1983; revised January 31, 1984. B. Soerowirdjo was supported by the British Council.

The authors are with the Department of Electronics, Southampton University, Southampton, Hants, S09 5NH, England.

Although considerable work has been published on the theoretical aspects of polysilicon emitter transistors, relatively little has been published on the experimental characteristics of these devices. In order to rectify this deficiency, in this paper, we present the results of detailed electrical measurements on different types of polysilicon emitter bipolar transistor. A comprehensive comparison is made with the theories from the literature in order to determine under which circumstances the alternative theories are valid. To assist with this comparison we have fabricated two types of polysilicon emitter transistor with identical processing except for the surface treatment prior to polysilicon deposition. Measurements of the temperature dependence of the gain are made on these devices over a wide range of temperatures, and a comparison made with the dependences predicted by the various theories.

II. Theory

In a previous paper, Eltoukhy and Roulston [15] presented a unified theory for current transport in polysilicon emitter bipolar transistors. A complete set of transport and tunneling equations was derived and arranged in such a way as to be suitable for fast numerical solution. In this paper, we present a simplified analytical version of this theory which is in a form suitable for comparison with experimental results. In this way, we are more easily able to identify the physical mechanisms that are controlling the operation of the different types of polysilicon emitter transistor.

Fig. 1 shows the band diagram of a polysilicon emitter transistor with a thin insulating layer between the polycrystalline and monocrystalline regions. This band diagram is a simplified version of that used in the full unified theory, and has been derived by making the following additional approximations. Firstly, it has been assumed that the emitter-base junction is extremely shallow so that recombination in the single-crystal part of the emitter can be ignored. This assumption is valid as long as the emitter depth below the polysilicon-silicon interface is small compared with the diffusion length of holes in the single-crystal part of the emitter. Crude calculations have shown that, for a junction depth of 0.04 μm and for a typical emitter profile, recombination in the single-crystal part of the emitter provides approximately 13 percent of the base current [17]. Secondly, we have assumed that there is no band bending at the polysilicon-silicon interface. The pub-

0018-9383/84/0700-0853$01.00 © 1984 IEEE

Authorized licensed use limited to: Sidley Austin LLP. Downloaded on May 15,2024 at 03:07:33 UTC from IEEE Xplore. Restrictions apply.

REC Exhibit 1023, Page 1 of 8

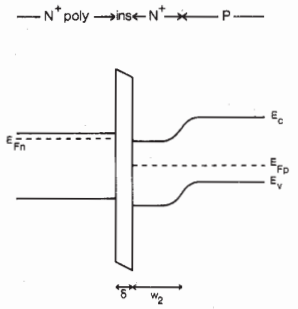

Fig. 1. Band diagram for a polysilicon-emitter bipolar transistor with a thin interfacial oxide layer.

lished models [18], [19] for conduction in polysilicon assume that the bands bend upwards in the vicinity of the grain boundary. This is caused by the trapping of carriers at the high concentration of defects and dangling bonds located at the grain boundary. As a result, the silicon adjacent to the grain boundaries becomes depleted of carriers and a potential barrier is formed. This barrier can be quite large in lightly doped polysilicon, but in heavily doped material it is negligible. For example, for a typical emitter doping concentration of 10^{19}–10^{20} cm^{-3}, and an interface state density of 10^{12} $cm^{-2} \cdot eV^{-1}$, the band bending is less than 1 meV [20].

The tunneling current is derived from the one-dimensional time-independent tunneling probability, which is given by [15]

$$D(E_x) = \exp\left[-\frac{4\pi}{h}\int_{x_1}^{x_2} [2m_i^*(qV(x) - E_x)]^{1/2}\, dx\right] \quad (1)$$

where $V(x)$ is the barrier height and E_x is the energy component of the incident carriers in the x direction. Assuming that the potential barrier is approximately rectangular with a height χ_h, the preceding integral can be evaluated to give

$$D(E_x) = \exp\left[-\frac{4\pi}{h}(2m_i^*)^{1/2}\,\delta\,(q\chi_h + E_x)^{1/2}\right]. \quad (2)$$

At this point in the analysis, the first two terms in the Taylor series expansion of $(1 + E_x/q\chi_h)^{1/2}$ are taken to give

$$D(E_x) = \exp\left[-\frac{4\pi}{h}(2m_i^*)^{1/2}\,\delta\,(q\chi_h)^{1/2}\left(1 + \frac{E_x}{2q\chi_h}\right)\right]. \quad (3)$$

The hole tunneling current density can then be derived as follows:

$$J_{pT} = J_B = q\left(\frac{kT}{2\pi m_h^*}\right)^{1/2}\frac{n_{ie}^2}{N_{de}}\,\frac{\exp - b_h}{(1 - C_h kT)}\exp\frac{qV_j}{kT} \quad (4)$$

where

$$C_h = \frac{2\pi\delta}{h}\left(\frac{2m_h^*}{q\chi_h}\right)^{1/2} \quad (5)$$

and

$$b_h = \frac{4\pi\delta}{h}(2m_h^* q\chi_h)^{1/2}. \quad (6)$$

The major difference between this equation and that derived by De Graaff and De Groot [10] is the presence of the $(1 - C_h kT)$ term in the denominator. This term did not arise in their analysis because the tunneling probability $D(E_x)$ was assumed to be a weak function of E_x and hence the E_x term in (3) was neglected [15].

The temperature dependence of the collector current density can be written as [10]

$$J_C(T) = \text{const}\,\frac{T^4}{\rho_b(T)}\exp -\frac{E_{gb}}{kT}\exp\frac{qV_j}{kT} \quad (7)$$

where $\rho_b(T)$ is the temperature dependence of the sheet resistance of the base under the emitter and is used to provide the temperature dependence of the mobility in the base. E_{gb} is the bandgap in the base. Using this equation together with (4) gives the following expression for the temperature dependence of the gain:

$$h_{FE}(T) = \text{const}\,\frac{T^{0.5}}{\rho_b(T)}(1 - C_h kT)\exp -\frac{(\Delta E_{ge} - \Delta E_{gb})}{kT} \quad (8)$$

where ΔE_{ge} and ΔE_{gb} are the bandgap narrowing in the emitter and base, respectively.

In the case where the insulating layer at the polysilicon-silicon interface is absent, the base current is determined by hole transport in the polycrystalline and monocrystalline regions of the emitter. The analysis for this type of device can be simplified if it is assumed that there is only one grain of polysilicon between the polysilicon-silicon interface and the metal contact. This assumption is supported by cross section TEM observations [5] which indicate that the polysilicon grains in this type of device are columnar in shape and extend completely through the polysilicon layer. Under these conditions, the full unified theory reduces to the analysis of Ning and Isaac [9]. The base current density is therefore given by

$$J_B = \frac{qD_{p2}n_{ie}^2}{W_2 N_{de}}\left[1 + \frac{D_{p2}}{D_{p1}}\,\frac{L_{p1}}{W_2}\right]^{-1}\exp\frac{qV_j}{kT} \quad (9)$$

where the subscripts 1 and 2 refer to the polycrystalline and monocrystalline regions of the emitter, respectively. Using (9) and (7), the temperature dependence of the gain can be written as

$$h_{FE}(T) = \frac{\text{const}}{\rho_b(T)}\left[1 + \frac{D_{p2}(T)}{D_{p1}(T)}\,\frac{L_{p1}(T)}{W_2}\right] \cdot \exp -\frac{(\Delta E_{ge} - \Delta E_{gb})}{kT}. \quad (10)$$

L_{p1} is the hole lifetime in the polysilicon and is given by

$$L_{p1} = (D_{p1}\tau_{p1})^{1/2}. \quad (11)$$

In heavily doped silicon, the hole lifetime τ_{p1} is limited by Auger recombination [21], [22] as follows:

$$\tau_{p1} = \frac{1}{C_n N_{de}^2} \quad (12)$$

Authorized licensed use limited to: Sidley Austin LLP. Downloaded on May 15,2024 at 03:07:33 UTC from IEEE Xplore. Restrictions apply.

REC Exhibit 1023, Page 2 of 8

where $C_n = 1.6 - 3 \times 10^{-31}$ cm$^6 \cdot$ s^{-1} is the Auger coefficient. τ_{p1} is therefore independent of temperature, and the temperature dependence of L_{p1} is determined by D_{p1} as follows:

$$D_{p1} = \frac{kT}{q} \mu_{p1}(T). \tag{13}$$

It is well known that, at high doping concentration, the mobility in single-crystal silicon is approximately independent of temperature [23]. However, for heavily-doped polysilicon, Seto [24] has observed that the hole mobility decreases significantly with increasing temperature, and can be described as follows:

$$\mu_{p1}(T) = \text{const } T^{-0.5} \exp - \frac{q\phi_{gb}}{kT} \tag{14}$$

where ϕ_{gb} is the barrier height at the polysilicon grain boundary. For heavily doped polysilicon, this barrier height is less than 1 meV, and hence the exponential term in (14) can be ignored. Making this approximation and using (10), (11), and (13) gives the following expression for the gain as a function of temperature:

$$h_{FE} = \text{const } \frac{1 + AT^{0.75}}{\rho_b(T)} \exp - \frac{(\Delta E_{ge} - \Delta E_{gb})}{kT} \tag{15}$$

where A is a constant which can be calculated from (10).

III. Experimental Procedure

Two types of polysilicon emitter bipolar transistors have been fabricated with identical processing except for the surface treatment prior to polysilicon deposition. The first type (HF devices) was given a dip etch in buffered hydrofluoric acid, which was intended to remove any native oxide which might have been present prior to polysilicon deposition. The second type (RCA devices) was given a dip etch in buffered HF followed by an RCA clean, and this was intended to grow an interfacial oxide layer of known thickness. Auger electron spectroscopy experiments have shown that a dip etch in buffered HF leaves an oxide layer of less than 2 Å [25], while an RCA clean produces an oxide film between 13 and 15 Å thick [26]. Although there is some doubt about the absolute values of these interfacial layer thicknesses, these results do show that the interfacial layer produced by the RCA clean is considerably thicker than that produced by the HF etch. This was confirmed in our work by the observation that slices given the HF etch were hydrophobic while those given the RCA clean were hydrophilic.

The interfacial layer treatments were immediately followed by the deposition of approximately 0.4 μm of undoped LPCVD polysilicon. The emitters of the transistors were then formed by implanting 1×10^{16} cm^{-2} arsenic into the polysilicon and driving-in at 900°C in wet oxygen.

Detailed electrical measurements were carried out on the two types of transistors including measurements of collector and base current as a function of base emitter voltage and the temperature dependence of the gain and resistance under the emitter.

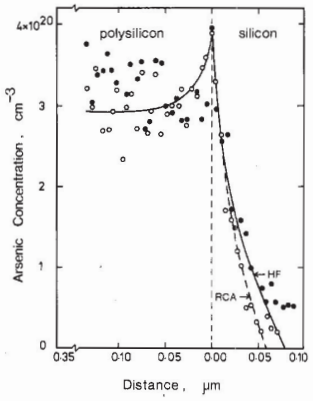

Fig. 2. Arsenic profiles, obtained from Rutherford backscattering experiments, for samples given an HF etch and an RCA clean.

The measurements as a function of temperature were carried out in an Oxford Instruments cryostat, type DN70, and in an oven for temperatures greater than 80°C. Measurements were made over the range -115 to +140°C at intervals of approximately 7°C. A full set of base and collector current-voltage characteristics was taken at each temperature, together with a measurement of the resistance under the emitter. The electrical measurements were supplemented with beveling and staining to provide the junction depths and Rutherford backscattering [27] to provide the arsenic profiles.

IV. Results

Fig. 2 shows the arsenic profiles, obtained from Rutherford backscattering experiments for the two types of surface treatment. The main feature of these profiles is the presence of a peak in the arsenic concentration at the polysilicon-silicon interface followed by a rapid decrease in the arsenic concentration on entering the single-crystal silicon. The arsenic peak has been reported previously [28] and explained by arsenic segregation at the grain boundaries. Another feature of the profiles in Fig. 2 is that the arsenic has penetrated slightly deeper into the silicon for the HF samples than for the RCA samples, though the resolution of Rutherford backscattering (≅300 Å) is such that this small difference may not be significant. However, similar results have been reported previously [28] for samples given stronger drive-ins, and were explained by retardation of the arsenic diffusion by the interfacial oxide layer.

The junction depths obtained from bevelling and staining are summarized in Table I, along with the results of the resistance under the emitter and gain measurements. The value of 0.04 μm for the emitter-base junction depths is in reasonable agreement with the arsenic profiles, considering the $\mp$0.03-μm error associated with the beveling and staining technique. The results in Table I indicate that, apart from the measured gains, the two types of transistor are very nearly identical. The small difference in the mean value of the resistance under the emitter indicates that the Gummel number [29] in the base of the RCA device is slightly higher than that in the HF device, suggesting that the arsenic atoms have penetrated deeper in the

Authorized licensed use limited to: Sidley Austin LLP. Downloaded on May 15,2024 at 03:07:33 UTC from IEEE Xplore. Restrictions apply.

REC Exhibit 1023, Page 3 of 8

TABLE I

DEVICE TYPE	E/B JUNCTION DEPTH μm	BASEWIDTH μm	RESISTANCE UNDER THE EMITTER kΩ/sq	GAIN
HF	0.04	0.25	5.6 ∓ 3.1	33 ∓ 2
RCA	0.04	0.25	4.3 ∓ 2.1	146 ∓ 15

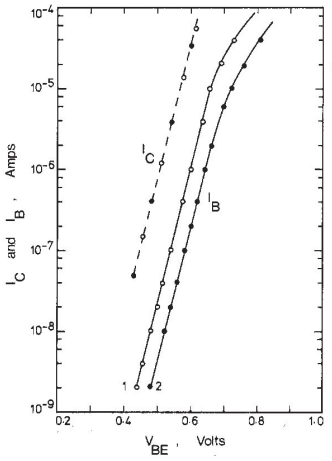

Fig. 3. Collector and base current as a function of base/emitter voltage for a device given an HF etch (device 1), and a comparable device given an RCA clean (device 2).

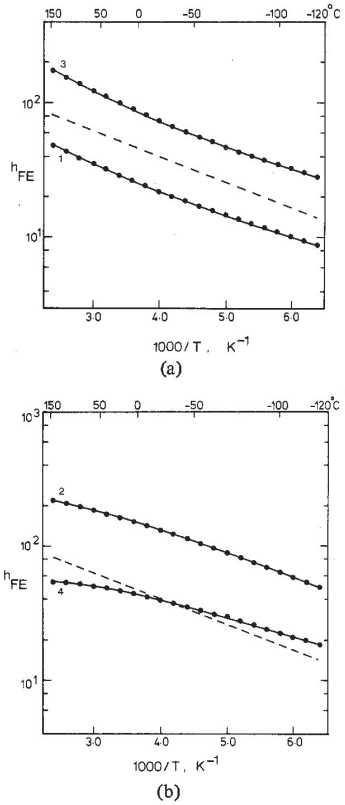

Fig. 4. Temperature dependence of the current gain for (a) two HF devices (transistors 1 and 3) and a conventional transistor (dashed line) and (b) two RCA devices (transistors 2 and 4) and a conventional transistor (dashed line).

HF device. This correlates well with the arsenic profiles in Fig. 2.

The major difference between the two types of device summarized in Table I is the value of gain obtained. In particular the RCA device has a gain approximately five times higher than that of the HF device. Similar results have been reported previously [8], and hence we can see that the properties of polysilicon emitter transistors are strongly influenced by the type of surface treatment carried out prior to polysilicon deposition. In addition, since apart from the interfacial layer treatment, the two types of device have had identical processing; we can infer that the physical mechanism controlling the gain is different for the two devices.

In order to facilitate a comparison with the theory, two transistors with identical values of resistance under the emitter (4.7 kΩ/sq) were selected from the large number of transistors measured and a more detailed electrical characterization carried out. Fig. 3 shows a graph of base and collector versus base-emitter voltage for these two devices. The characteristics for both devices are ideal with an exp qV_{BE}/kT dependence over four decades of current. As expected, the collector characteristics of the two devices are identical, and the improved gain of the RCA device arises because of a decrease in the base current.

Fig. 4(a) shows a graph of current gain as a function of temperature for two HF devices and for a conventional transistor for comparison. The gain was calculated from the ideal part of the I_C and I_B versus V_{BE} characteristics at each temperature. Measurements above 140°C were not possible because of excessive collector leakage and below −115°C because the base characteristics were not ideal. The conventional device is a BFY50, general-purpose n-p-n switching transistor, device 1 is the HF device presented in Fig. 3, and device 3 is an HF device processed at a different time, under different processing conditions. It can be seen that the characteristic for the conventional device is linear, which is as expected for this type of device. In contrast, the characteristics for the two HF devices are nonlinear, with the gain increasing more rapidly with temperature at high temperatures.

Fig. 4(b) shows the temperature dependence of the gain for two RCA devices and the conventional transistor for comparison. The upper characteristic (device 2) is for the RCA device presented in Fig. 3 and the lower characteristic (device 4) is for a device processed at a different time, under different processing conditions. The characteristics for the two RCA devices are again nonlinear, but the shapes of the characteristics are significantly different than those obtained for the HF devices in Fig. 4(a). At low temperatures the characteristics of the RCA and HF devices have similar slopes, but at high temperatures the rate of increase of gain with temperature shows a marked decrease for the RCA devices, whereas the opposite occurs for the HF devices. This effect is particularly noticeable in device 4.

Authorized licensed use limited to: Sidley Austin LLP. Downloaded on May 15,2024 at 03:07:33 UTC from IEEE Xplore. Restrictions apply.

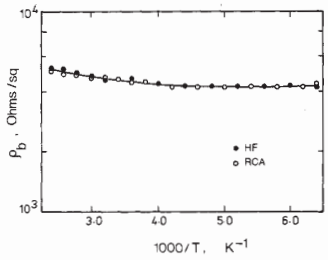

Fig. 5. Temperature dependence of the resistance under the emitter for the RCA and HF devices.

Fig. 5 shows the temperature dependence of the resistance under the emitter for the two types of device. These measurements were made on four terminal pinch resistors located adjacent to the transistors under test. It can be seen that the two types of device have identical characteristics, and that the resistance is approximately flat over the temperature range of the measurements.

V. Comparison of Experimental Results and Theory

A. HF Devices

The purpose of this section is to explain the shape of the graph of h_{FE} versus $1000/T$ for the HF devices and hence determine which theory is applicable to these devices. The first stage of the analysis is to obtain measurements of the bandgap narrowing in the base and emitter regions of the transistor. From (7), the bandgap in the base E_{gb} can be obtained from the slope of a graph of $\ln I_{C0}\rho_b/T^4$ versus inverse temperature as shown in Fig. 6. The bandgap narrowing in the base ΔE_{gb} can be obtained by subtracting the bandgap in the base E_{gb} from the bandgap for undoped silicon extrapolated to 0 K (1206 meV) [30]. The value of bandgap narrowing obtained from this analysis is $\Delta E_{gb} = 74 \mp 10$ meV.

In order to confirm that the preceding value is reasonable for our devices, it is possible to extract the base doping concentration from the measured bandgap narrowing using Slotboom's [30] formula and compare this with the theoretical base profile in our devices. Using this method, a boron concentration of 6×10^{18} cm^{-3} is obtained from our value of 74 meV for the bandgap narrowing in the base. Fig. 7 shows the theoretical boron profile obtained from the SUPREM process simulation program. This gives a peak base doping concentration of approximately 5×10^{18} cm^{-3} which is in good agreement with the value of 6×10^{18} cm^{-3} obtained from the bandgap narrowing data.

The bandgap narrowing in the emitter can be extracted from the temperature dependence of the gain, as plotted in Fig. 4. At temperatures below 240 K, the resistance under the emitter shown in Fig. 5 is constant, and hence its influence on the temperature dependence of the gain can be neglected. In addition in our devices, the $AT^{0.75}$ term in (15) is greater than unity since $D_{p2}/D_{p1} \cong 3$ [9] and $W_2 < L_{p1}$. The bandgap narrowing in the emitter can therefore be obtained from the slope, measured at low temperatures, of a graph of $\ln h_{FE}/T^{0.75}$ versus inverse temperature. Using this method a value of 96 ∓ 13 meV is obtained for the bandgap narrowing in the emitter for the HF device.

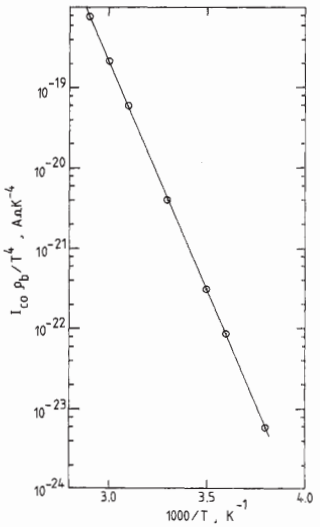

Fig. 6. Graph of $\ln I_{C0}/T^4$ versus inverse temperature for the RCA and HF devices.

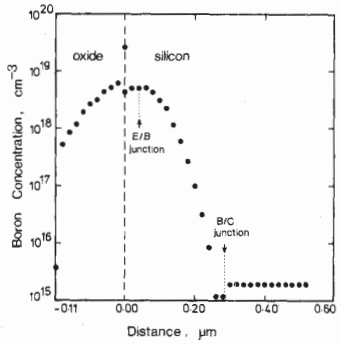

Fig. 7. Theoretical boron profile obtained from the SUPREM process simulation program.

Values of bandgap narrowing in the emitter ranging from 70 to 170 meV [30]-[32] have been reported in the literature for various types of bipolar transistors. In order to explain this wide spread in experimental results, theoretical models have been proposed by Van Overstraeten *et al.* [33], Lanyon and Tuft [34], and Slotboom and de Graaff [30] which relate the bandgap narrowing to the emitter concentration at high doping levels. Using these models we obtain an emitter concentration of between 1.8 and 5.0×10^{19} cm^{-3} for our value of 96 meV for the bandgap narrowing in the emitter. The arsenic profiles shown in Fig. 2 indicate that the arsenic concentration in the polysilicon is approximately 3×10^{20} cm^{-3}. However, Rutherford backscattering gives the total arsenic concentration, and we would expect the electrically active concentration to be considerably lower. Ryssel *et al.* [35] have compared the total arsenic concentration in ion-implanted polysilicon (1×10^{16} cm^{-2} at 90 keV) obtained from Rutherford backscatter-

Authorized licensed use limited to: Sidley Austin LLP. Downloaded on May 15,2024 at 03:07:33 UTC from IEEE Xplore. Restrictions apply.

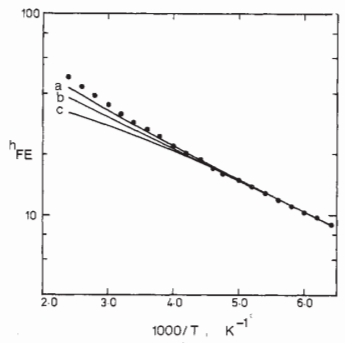

Fig. 8. Fit obtained between the transport theory (15) and the experimental results (HF device 1) for $AT^{0.75} \gg 1$ (curve *a*), $AT^{0.75} \ll 1$ (curve *c*), and for an intermediate case, (curve *b*).

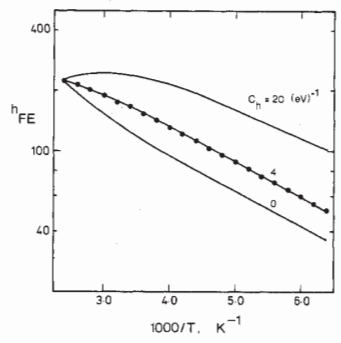

Fig. 9. Fit obtained between the modified tunneling theory (8) and the experimental results (RCA device 2) for three values of the parameter C_h.

ing with the electrically active concentration obtained from Hall effect measurements. They found, after a drive-in schedule of 30 min at 950°C, that only 25–30 percent of the arsenic was electrically active. In our devices, the emitter drive-in was 20 min at 900°C, and hence we would expect an even smaller proportion of the arsenic to be electrically active. Taking into account this information, the value of 96 meV for the bandgap narrowing in the emitter is not unreasonable. Further confirmation of this point can be obtained by considering the emitter–base junction depth of 0.04 μm, and comparing this with the mean polysilicon grain size. Cross section TEM observations [5] have shown that, in our devices, the mean grain size is between 0.1 and 0.2 μm. We can therefore see that the arsenic is unlikely to have penetrated into the center of the grains, and hence we would not expect the electrical activity to be high.

Having obtained values for the bandgap narrowing in the base and emitter, we are now in a position to investigate how the other parameters in (15) influence the temperature dependence of the gain. In order to do this we need to assume a value for the parameter A in (15). Fig. 8 shows a comparison of the theoretical and experimental gain versus inverse temperature for $AT^{0.75} \gg 1$, $AT^{0.75} \ll 1$, and for an intermediate case. It can be seen that the best agreement between theory and experiment is obtained for $AT^{0.75} \gg 1$. Since Ning and Isaac [9] have reported that $D_{p2}/D_{p1} \cong 3$, this implies that $L_{p1} \gg W_2$. Assuming an emitter doping concentration of 5×10^{19} cm^{-3}, as obtained from the bandgap narrowing in the emitter measurements, and using (11) and (12) with $D_{p1} = 0.43$ cm$^2 \cdot$s^{-1} [9], [36] we obtain $L_{p1} > 0.24$ μm. This value is therefore consistent with the criterion that $AT^{0.75} \gg 1$.

The agreement between theory and experiment shown in Fig. 8 is excellent at low temperatures but somewhat poorer at high temperatures. A perfect fit with theory can be obtained if the $T^{0.75}$ term in (15) is replaced by a $T^{1.0}$ term. This small discrepancy between the experimental and theoretical results indicates that an additional temperature dependent term is present which has not been included in (15). The most likely cause of this discrepancy is that the temperature dependence of the mobility in the base or in the polysilicon has not been correctly described. In particular, the mobility in the polysilicon quoted in (14) is for majority carriers [24], whereas in the emitter of our device the holes are minority carriers. Alternatively it might be explained by oversimplification in deriving (15), since we have not made allowance for possible differences in doping concentration in the polycrystalline and single-crystalline parts of the emitter or for the nonuniform doping concentration in the base.

B. RCA Devices

The first stage of this analysis is again to obtain measurements for the bandgap narrowing in the base and emitter. As with the HF device, the bandgap narrowing in the base is obtained from the temperature dependence of the collector current as shown in Fig. 6. The value obtained is 74 ∓ 10 meV which, as expected, is identical to that obtained for the HF device. The bandgap narrowing in the emitter can be obtained from the temperature dependence of the gain as described by (8). At low temperatures ($1000/T > 4.5$) the $C_h kT$ term in (8) is small with respect to unity and the resistance under the emitter is constant. Consequently the bandgap narrowing in the emitter can be obtained from the slope of a graph of $\ln h_{FE}/T^{0.5}$ versus inverse temperature. This gives a value of 101 meV which, as expected, is close to the value of 96 meV obtained for the HF devices.

Having obtained values for the bandgap narrowing in the base and emitter we are now in a position to fit our modified tunneling theory to the experimental results for the RCA device. Fig. 9 shows a comparison of theoretical and experimental gain versus inverse temperature for three values of the parameter C_h in (8). It can be seen that an excellent fit can be obtained for a value of $C_h = 4$ eV^{-1}. This parameter depends upon the interfacial layer thickness δ and the effective barrier height for holes χ_h, and hence from the measured value of δ we should be able to obtain an estimate for χ_h. Henderson [26] used Auger electron spectroscopy to measure the thickness of oxide produced by the RCA clean and obtained a value of approximately 14 Å. If we insert this value into (5) we obtain 500 meV for the effective barrier height for holes. Ng and Card [37] have measured the hole and electron tunneling barriers on MOS structures with ultrathin (<40 Å)

Authorized licensed use limited to: Sidley Austin LLP. Downloaded on May 15,2024 at 03:07:33 UTC from IEEE Xplore. Restrictions apply.

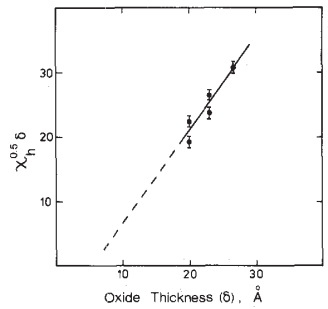

Fig. 10. Graph, taken from the literature [37], showing the relationship between the effective barrier height for holes and the interfacial oxide thickness.

oxide layers, and their data is summarized in Fig. 10. Extrapolating their results to an oxide thickness of 14 Å gives an effective barrier height for holes of approximately 700 meV, which is in good agreement with the value of 500 meV obtained from our electrical measurements. In our finished transistors it is likely that the oxide layer is thinner than 14 Å since the devices were subjected to a high-temperature emitter drive-in, and Duffill [35] has shown that the oxide thickness decreases during high-temperature processing. This would have the effect of reducing the value of effective barrier height obtained from (5).

It is worth noting at this point that the measurements of Ng and Card [37] indicate that the effective barrier height for electrons is very much smaller than that for holes. Qualitatively, this means that the tunneling probability is very much higher for electrons than holes, and consequently electrons can penetrate the oxide barrier more easily. The significance of this for polysilicon emitter transistors is that the base current is suppressed, but the emitter current is not. This explains why very little voltage is dropped across the interfacial oxide.

The modified tunneling theory summarized in (8) and Fig. 9 predicts that the gain should decrease with temperature at very high temperatures and for very thick interfacial oxides. In our devices, measurements at temperatures >420 K could not be made because of excessive collector leakage. However, in an attempt to observe this effect we have made measurements on a number of RCA devices processed at different times. The characteristic for device 4 in Fig. 4(b) shows a very strong decrease in the rate of increase of the gain at high temperatures, and at temperatures above 350 K the gain is very nearly constant. In addition de Graaff and de Groot [10] reported that in some cases the temperature coefficient of the gain of their polysilicon emitter transistors was negative. This result can readily be explained using the modified tunneling theory.

VI. Conclusions

In conclusion, we have shown that the electrical characteristics of polysilicon emitter transistors are extremely sensitive to the type of surface treatment given prior to polysilicon deposition. In particular, transistors given an RCA clean have gains approximately five times higher than transistors given an etch in buffered hydrofluoric acid. The temperature dependence of the gain is different for the two types, with the HF devices exhibiting a much stronger dependence at high temperatures than the RCA devices. The electrical characteristics of the RCA devices can be fully explained using the modified tunneling theory of Eltoukhy and Roulston [15]. The electrical characteristics of the HF devices can largely be explained using the transport theory of Ning and Isaac [9], though a small modification is needed to the temperature dependence of the gain.

Acknowledgment

The authors would like to thank the Science and Engineering Research Council and Surrey University for providing access to the Rutherford backscattering facilities. Special thanks are due to Prof. D. J. Roulston and Dr. A. A. Eltoukhy of Waterloo University, Canada, for many stimulating and helpful discussions. We would also like to express our gratitude to Dr. A. G. R. Evans for advice on the temperature measurements, and the staff of the Southampton University Microelectronics Centre for assistance with the fabrication of the devices. We would also like to thank Dr. P. Ward and Mrs. J. Duffill of Plessey, Caswell, and Dr. G. R. Booker and Dr. M. Wilson of Oxford University for their advice and encouragement.

References

[1] D. D. Tang, T. H. Ning, R. D. Isaac, G. C. Feth, S. K. Wiedmann, and H. N. Yu, "Subnanosecond self-aligned I^2L/MTL circuits," *IEEE J. Solid-State Circuits*, vol. SC-15, pp. 444–449, 1980.

[2] T. H. Ning, R. D. Isaac, P. M. Solomon, D. D. Tang, H. N. Yu, G. C. Feth, and S. K. Wiedmann, 'Self-aligned bipolar transistors for high performance and low power delay VLSI," *IEEE Trans. Electron Devices*, vol. ED-28, pp. 1010–1013, 1981.

[3] T. Sakai, Y. Yamamoto, Y. Kobayashi, K. Kawarada, Y. Inabe, T. Hayashi, and H. Miyagana, "A 3-ns 1-kbit RAM using super self-aligned process technology," *IEEE J. Solid-State Circuits*, vol. SC-16, pp. 424–428, 1981.

[4] M. Finetti, G. Masetti, P. Negrini, and S. Solmi, "Predeposition through a polysilicon layer as a tool to reduce anomalies in phosphorous profiles and push-out effect in n-p-n transistors," in *IEE Proc.*, vol. 127, pt. I, pp. 37–41, 1980.

[5] M. C. Wilson, P. Ashburn, B. Soerowirdjo, G. R. Booker, and P. Ward, "TEM and RBS studies of the regrowth of arsenic implanted polysilicon due to an oxidation drive-in," *J. de Physique*, vol. C1, supp. 10, pp. C1 253–C1 257, 1982.

[6] A. Armigliato, M. Finetti, D. Nobili, M. Servidori, and Solmi, "Role of polysilicon in the reduction of defects and anomalous diffusion associated to phosphorous predeposition," in *Proc. 9th ESSDERC*, Sept. 1979.

[7] C. Bull, P. Ashburn, G. R. Booker, and K. H. Nicholas, "Effects of dislocations in silicon transistors with implanted emitters," *Solid-State Electron.*, vol. 22, pp. 95–104, 1979.

[8] B. Soerowirdjo and P. Ashburn, "Effects of surface treatments on the electrical characteristics of bipolar transistors with polysilicon emitters," *Solid-State Electron.*, vol. 26, pp. 495–498, 1983.

[9] T. H. Ning and R. D. Isaac, "Effect of emitter contact on current gain of silicon bipolar devices," *IEEE Trans. Electron Devices*, vol. ED-27, pp. 2051–2055, 1980.

[10] H. C. de Graaff and J. G. de Groot, "The SIS tunnel emitter: A theory for emitters with thin interface layers," *IEEE Trans. Electron Devices*, vol. ED-26, pp. 1771–1776, 1979.

[11] J. Graul, A. Glasl, and H. Murrman, "High-performance transistors with arsenic-implanted polysil emitters," *IEEE J. Solid-State Circuits*, vol. SC-11, pp. 491–495, 1976.

[12] B. Soerowirdjo, P. Ashburn, and A. Cuthbertson, "The influence of surface treatments on the electrical characteristics of polysilicon emitter bipolar transistors," in *IEDM Tech. Dig.*, pp. 668–671, 1982.

Authorized licensed use limited to: Sidley Austin LLP. Downloaded on May 15,2024 at 03:07:33 UTC from IEEE Xplore. Restrictions apply.

[13] J. G. Fossum and M. A. Shibib, "A minority carrier transport model for polysilicon contacts to bipolar devices, including solar cells," in *IEDM Tech. Dig.*, pp. 280–283, 1980.
[14] P. H. Yeung and W. C. Ko, "Current gain in polysilicon emitter transistors," *IEEE Trans. Electron Devices*, vol. ED-30, pp. 593–597, 1983.
[15] A. A. Eltoukhy and D. J. Roulston, "The role of interfacial layer in polysilicon emitter bipolar transistors," *IEEE Trans. Electron Devices*, vol. ED-29, pp. 1862–1869, 1982.
[16] ——, "Minority-carrier injection into polysilicon emitters," *IEEE Trans. Electron Devices*, vol. ED-29, pp. 961–964, 1982.
[17] A. A. Eltoukhy, private communication.
[18] M. M. Mandurah, K. C. Saraswat, and T. I. Kamins, "A model for conduction in polycrystalline silicon–Part I: Theory," *IEEE Trans. Electron Devices*, vol. ED-28, pp. 1163–1171, 1981.
[19] ——, "A model for conduction in polycrystalline silicon–Part II: Comparison of theory and experiment," *IEEE Trans. Electron Devices*, vol. ED-28, pp. 1171–1176, 1981.
[20] H. C. Card and E. S. Yang, "Electronic processes at grain boundaries in polycrystalline semiconductors under optical illumination," *IEEE Trans. Electron Devices*, vol. ED-24, pp. 397–402, 1977.
[21] J. Dziewior and W. Schmid, "Auger coefficients for highly doped and highly excited silicon," *Appl. Phys. Lett.*, vol. 31, pp. 346–348, 1977.
[22] D. K. Schroder, "The concept of generation and recombination lifetimes in semiconductors," *IEEE Trans. Electron Devices*, vol. ED-29, pp. 1336–1338, 1982.
[23] V. I. Fistul, *Heavily Doped Semiconductors*. New York: Plenum, 1969.
[24] J. W. Seto, "The electrical properties of polycrystalline silicon films," *J. Appl. Phys.*, vol. 46, pp. 5247–5254, 1975.
[25] J. E. Duffill, "An investigation of interfacial oxide thicknesses between silicon," in *Proc. 12th ESSDERC*, Sept. 1982.
[26] R. C. Henderson, "Silicon cleaning with hydrogen peroxide solutions: A high energy electron diffraction and Auger electron spectroscopy study," *J. Electrochem. Soc.*, vol. 119, pp. 772–775, 1982.
[27] D. V. Morgan, "Rutherford scattering analysis: A tool for semiconductor-device technology," *Solid-State Electron Devices*, vol. 1, pp. 37–45, 1977.
[28] P. Ashburn and B. Soerowirdjo, "Arsenic profiles in bipolar transistors with polysilicon emitters," *Solid-State Electron.*, vol. 24, pp. 475–476, 1981.
[29] H. K. Gummel, "Measurement of the number of impurities in the base layer of a transistor," *Proc. IRE*, vol. 49, p. 839, 1961.
[30] J. W. Slotboom and H. C. de Graaff, "Measurements of bandgap narrowing in Si bipolar transistors," *Solid-State Electron.*, vol. 19, pp. 857–862, 1976.
[31] W. L. Kauffmann and A. A. Bergh, "The temperature dependence of ideal gain in double diffused silicon transistors," *IEEE Trans. Electron Devices*, vol. ED-15, pp. 732–735, 1968.
[32] A. W. Wieder, "Emitter effects in shallow bipolar devices: Measurement and consequences," *IEEE Trans. Electron Devices*, vol. ED-27, pp. 1402–1408, 1980.
[33] R. J. Van Overstraeten, H.J.J. de Man, and R. P. Merten, "Transport equations in heavily doped silicon," *IEEE Trans. Electron Devices*, vol. ED-20, pp. 290–298, 1973.
[34] H.P.D. Lanyon and R. A. Tuft, "Bandgap narrowing in moderately to heavily doped silicon," *IEEE Trans. Electron Devices*, vol. ED-26, pp. 1014–1018, 1979.
[35] H. Ryssel, H. Iberl, M. Bleier, G. Prinke, K. Haberger, and H. Kranz, "Arsenic implanted polysilicon layers," *Appl. Phys.*, vol. 24, pp. 197–200, 1981.
[36] R. S. Muller and T. I. Kamins, *Device Electronics for Integrated Circuits*. New York: Wiley, 1977.
[37] K. K. Ng and H. C. Card, "Asymmetry in the SiO_2 tunneling barriers to electrons and holes," *J. Appl. Phys.*, vol. 51, pp. 2153–2157, 1980.

Authorized licensed use limited to: Sidley Austin LLP. Downloaded on May 15,2024 at 03:07:33 UTC from IEEE Xplore. Restrictions apply.